Association Between Optic Nerve Head Deformation and Retinal Microvasculature in High Myopia

MI SUN SUNG, TAE HEE LEE, HWAN HEO, AND SANG WOO PARK

• PURPOSE: To evaluate the retinal microvasculature of peripapillary and macular regions in highly myopic eyes and investigate the association between the vascular parameters and optic nerve head (ONH) deformation.
• DESIGN: Cross-sectional study.
• METHODS: Seventy-one subjects with highly myopic eyes and 26 subjects with emmetropic eyes were included. Horizontal B-scan images of the ONH were obtained using optical coherence tomography (OCT) and horizontal tilt angles were measured. Integrated automated algorithms in the Avanti OCT angiography were used to quantify the peripapillary vessel density and area of the foveal avascular zone (FAZ) at the level of superficial and deep vascular networks. Association between horizontal disc tilt and the vascular parameters was evaluated.
• RESULTS: The mean axial length and horizontal tilt angle were 26.73 ± 0.63 mm and 9.77 ± 3.00 degrees in the highly myopic group and 23.46 ± 0.55 mm and 5.95 ± 3.48 degrees in the emmetropic group, respectively. Highly myopic eyes exhibited significantly lower average peripapillary vessel density ($P = .010$) and larger superficial and deep FAZs ($P = .001$ and $P < .001$, respectively) compared with emmetropic eyes. Linear regression analyses showed that horizontal tilt angle significantly correlated the average peripapillary vessel density ($P = .037$) and the areas of superficial ($P < .001$) and deep ($P < .001$) FAZs.
• CONCLUSIONS: The retinal microvasculature was significantly different in highly myopic eyes according to the degree of horizontal optic disc tilt. In addition to peripapillary vessel density, FAZ can be affected by the degree of optic disc tilt. (Am J Ophthalmol 2018;188:81–90. © 2018 Elsevier Inc. All rights reserved.)

AJO.com Supplemental Material available at AJO.com.

Accepted for publication Jan 29, 2018.

From the Department of Ophthalmology and Research Institute of Medical Sciences, Chonnam National University Medical School and Hospital, Gwangju, South Korea (M.S.S., T.H.L., H.H., S.W.P.); and Center for Creative Biomedical Scientists, Chonnam National University, Gwangju, South Korea (S.W.P.).

Inquiries to Sang Woo Park, Department of Ophthalmology and Research Institute of Medical Sciences, Chonnam National University Medical School and Hospital, 42 Jebong-ro, Dong-gu, Gwangju 61469, South Korea; e-mail: exo70@naver.com

HIGH MYOPIA IS THOUGHT TO BE ASSOCIATED with decreased retinal perfusion. Avetisov and Savitskaya[1] performed a fluorescein angiography study and found that fluorescein transit times were delayed in high myopia. Shimada and associates[2] also described reduced retinal blood flow in highly myopic eyes using laser Doppler velocimetry. Similarly, several studies have reported narrowing of the retinal arteriolar and venular caliber or reduced retinal blood flow with axial length elongation.[3–6]

Spectral-domain optical coherence tomography (OCT) provides us the details of the optic nerve head (ONH) and retina.[7] Recently, the development of OCT angiography (OCTA) has enabled direct and noninvasive imaging of the retinal vasculature and several studies using OCTA have provided more detailed qualitative and quantitative microvascular information about myopic eyes.[8–13] From these studies, it has gradually become clear that retinal microvascular density can be altered in both superficial and deep vascular plexuses with axial length elongation.

Among microvascular parameters in the retina, the foveal avascular zone (FAZ) is a specialized and capillary-free region in the macula that has the highest cone photoreceptor density.[14,15] Since the FAZ is surrounded by an interconnected capillary bed, it is affected by changes of the retinal microvasculature in the macula and known to be one of the important parameters of circulatory state for the central retina. Therefore, the FAZ has been thought to have significant diagnostic and prognostic value in various retinal diseases.[16] Recently, Kwon and associates[17] demonstrated the clinical significance of FAZ as a predictor of central visual field (VF) defect in glaucoma. In this regard, given the high prevalence of retinal diseases and glaucoma in myopic eyes, it would be useful to know how the FAZ varies among the myopic individuals. However, the FAZ in myopic eyes has been studied in less detail.

Characteristic deformations of the ONH in myopic eyes, such as optic disc tilt, optic disc rotation, and β-zone peripapillary atrophy (PPA), are results of posterior scleral remodeling during axial elongation.[18–21] In the current study, we hypothesized that myopia-related ONH deformation might be associated with the retinal microvasculature. Therefore, the aim of the present study was to evaluate the microvasculature of the peripapillary region and FAZ in

0002-9394/$36.00
https://doi.org/10.1016/j.ajo.2018.01.033

highly myopic eyes, using OCTA, and to investigate the association between ONH deformation and these vascular parameters.

METHODS

• **SUBJECTS:** This prospective, cross-sectional study adhered to the tenets of the Declaration of Helsinki and was approved by the Institutional Review Board of the Chonnam National University Hospital. The participants were informed of the study objectives and written informed consent was obtained from all participants.

Healthy volunteers were prospectively and consecutively recruited from July 1 2016 to September 31, 2016. In an effort to study the characteristics of high axial myopia without any pathologic changes in the ONH or retina, only eyes with an axial length between 26 and 28 mm were included. The control group had emmetropic eyes with mean spherical equivalent (SE) refractive error between 0.5 and −0.5 diopters (D) and axial length between 22 and 24 mm. All subjects underwent complete ophthalmic examination, including measurement of best-corrected visual acuity (BCVA), intraocular pressure (IOP) using Goldmann applanation tonometry, manifest refraction, slit-lamp examination, ONH and peripapillary retinal nerve fiber layer (pRNFL) examination using color stereoscopic disc photography and red-free RNFL fundus photography, and the Swedish Interactive Threshold Algorithm standard 30-2 perimetry with a Humphrey Field Analyzer (Carl Zeiss Meditec Inc, Dublin, California, USA). All IOP measurements were recorded between 4:00 PM and 7:00 PM. Axial length and central corneal thickness were measured using optical low-coherence reflectometry (Lenstar; Haag-Streit AG, Koeniz, Switzerland). A detailed medical history was recorded for each subject.

The following inclusion criteria were used: healthy subjects aged between 20 and 30 years, astigmatism within ±2 D, BCVA of 20/25 or better, IOP ≤ 21 mm Hg, nonglaucomatous healthy ONHs on stereoscopic photographs (an intact neuroretinal rim without peripapillary hemorrhage, thinning, or localized pallor), absence of any RNFL abnormalities on red-free fundus photographs, and normal VF results in both eyes. Patients with a family history of glaucoma in a first-degree relative, history of intraocular or refractive surgery, pathologic myopia (patch chorioretinal atrophy, lacquer crack lesions, intrachoroidal cavitations, choroidal neovascularization), other evidence of retinal pathology, or opaque media were excluded. For cases in which both eyes of a subject met the inclusion criteria, only 1 eye was chosen randomly.

• **EVALUATION OF OPTIC NERVE HEAD:** Digital retinal photographs centered on the optic disc and macula were obtained using standard settings with a nonmydriatic retinal camera. Each photograph was exported to a desktop computer as a TIFF image file. Using public-domain Java-based image processing software developed by the National Institutes of Health (ImageJ, Version 1.4.1; Wayne Rasband; National Institutes of Health, Rockville, Maryland, USA), ovality index, areas of the optic disc and β-zone PPA, and cup-to disc area ratio were measured by 2 independent examiners (M.S.S. and H.H.). Averaged data were used in the final analyses.

The measurement of ovality index has been previously described.[22,23] Briefly, ovality index is defined as the ratio between the longest and shortest diameters of the optic disc. The areas of the optic disc and β-zone PPA were determined as the total number of pixels using ImageJ software in a circumferential pattern. Combined with a fundus camera magnification factor of 1.4×, the total magnification by the camera and ImageJ system was calculated. We converted the area from pixels to mm^2. The area was corrected using Littmann's formula for each axial length.[24] The anterior corneal curvature radius was set at 7.8 mm, which is the reported mean for white and Chinese individuals.[25]

• **SPECTRAL-DOMAIN OPTICAL COHERENCE TOMOGRAPHY IMAGING:** All subjects underwent traditional ONH and macular imaging with Avanti spectral-domain OCT (RTVue-XR Avanti; Optovue, Fremont, California, USA). The ONH map protocol calculated pRNFL thickness in a 10-pixel-wide band along a 3.45-mm-diameter circle centered on the optic disc. The overall average pRNFL thickness was measured, and then the effect of ocular magnification was corrected by the method of Kang and associates.[26] Corrected average pRNFL thickness was used for the final analysis. Foveal thickness was also measured on 3 × 3-mm scans centered on the fovea. The fovea was defined as the area within the central 1-mm ring of the Early Treatment Diabetic Retinopathy Study grid. The full retinal layer thickness was defined by the algorithm as the distance between the internal limiting membrane (ILM) and the middle of the retinal pigment epithelium (RPE).

• **MEASUREMENT OF HORIZONTAL OPTIC DISC TILT:** The horizontal tilt angle of the optic disc was measured in accordance with the previously described method from horizontal cross-sectional OCT images.[27,28] Optic disc margins on scanning laser ophthalmoscopy images were delineated and marked on the corresponding cross-sectional OCT images, where they met the Bruch membrane or border tissue. A line connecting these 2 points, marking the clinical disc margins, was considered as the ONH plane. Another line connecting the inner tips of the Bruch membrane, on each side of the ONH, was defined as the reference plane. The degree of horizontal tilt was defined as the angle between the reference plane and the ONH plane (Figure 1, Left). Measurements were

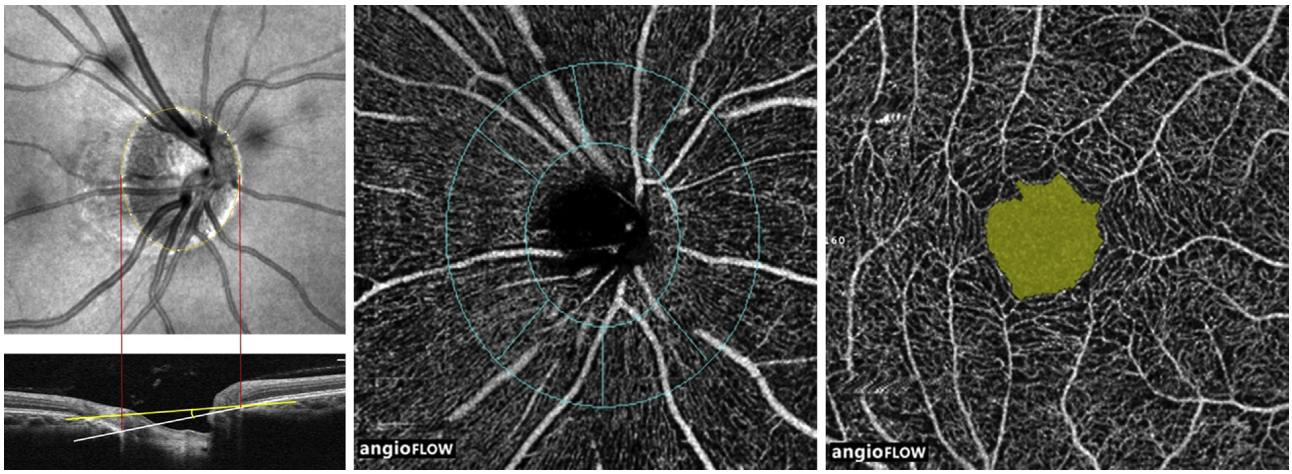

FIGURE 1. Measurement of horizontal tilt angle and vessel density. (Left) Optic disc boundaries were delineated on the scanning laser ophthalmoscopy images. Points at which the disc borders met the Bruch membrane or border tissue were marked on the corresponding cross-sectional optical coherence tomography (OCT) image. A white line connecting the 2 points, marking the clinical boundary of the disc, was defined as the optic nerve head (ONH) plane. A yellow line, connecting the inner edges of the Bruch membrane on each side of the ONH, was considered the reference plane. Degree of horizontal disc tilt was measured from the angle between the reference and ONH planes. (Center) Average peripapillary vessel density was calculated within a 750-μm-wide elliptical annulus, extending outward from the ONH boundary from the radial peripapillary capillary segment. (Right) An automated software algorithm integrated into the OCT angiography system graphically highlighted and calculated the foveal avascular zone (FAZ) areas from superficial and deep vascular networks.

made by 2 independent examiners (M.S.S. and H.H.), and averaged data were used in the final analyses.

• **MEASUREMENT OF SUBFOVEAL CHOROIDAL THICKNESS:** Subfoveal choroidal thickness was evaluated by the enhanced depth imaging (EDI) technique of the Avanti spectral-domain OCT device. From the 12-mm-length EDI scan running through the fovea, vertical distance from the hyper-scattering outer border of the RPE to the inner border of the sclera at the center of the fovea was measured and it was defined as subfoveal choroidal thickness. Images with signal strength below 60 or cases in which RPE and choriosclera interface were not clearly identified were excluded from the analysis. The average of data from 2 independent examiners (M.S.S. and H.H.) was used in this study.

• **OPTICAL COHERENCE TOMOGRAPHY ANGIOGRAPHY IMAGING:** The AngioVue incorporated in Avanti spectral-domain OCT was used for angiography imaging. Using a light source (centered on 840 nm, bandwidth of 45 nm), Avanti OCT performed an A-scan at a rate of 70-kHz scans per second. The scans were acquired over a 4.5 × 4.5-mm region centered on the optic disc and a 3 × 3-mm region centered on the fovea. Two volumetric raster scans, including 1 horizontal priority (x-fast) and 1 vertical priority (y-fast), were obtained consecutively in approximately 3 seconds. To identify perfused vessels, the volumetric scans were processed using split-spectrum amplitude-decorrelation angiography (SSADA) algorithms. Any motion artifacts were removed using 3-dimensional orthogonal registration and merging of the 2 scans. Details regarding Avanti OCT and the SSADA algorithms are described in previous studies.[29]

The AngioVue disc mode automatically segmented the optic disc into 4 layers: ONH, vitreous, radial peripapillary capillary (RPC), and choroid. For the measurement of superficial peripapillary microvascular density, the RPC segment extending from the ILM to the RNFL was analyzed. Vessel density is defined as the percentage area occupied by vessels in a given region. The software automatically fitted an ellipse to the optic disc margin and calculated the average vessel density around the optic disc. After the accuracy of the optic disc margin was reviewed, the line was adjusted manually, and average peripapillary vessel density was measured in the region defined as a 0.75-mm-wide elliptical annulus extending from the optic disc boundary (Figure 1, Center).

Measurements of the FAZ area were performed using the non-flow function of the OCTA software, at the level of the superficial and deep vascular networks (Figure 1, Right). The boundaries of the superficial network extended from 3 μm below the ILM to 15 μm below the inner plexiform layer (IPL). The deep capillary network extended from 15 μm to 70 μm below the IPL. For assessing the dimensional information of the retina, such as FAZ area in high myopia, correcting for ocular magnification should be considered.[30] Therefore, Bennett's formula was used to determine a scaling factor for the OCT angiogram.[24] The relationship between the OCT image measurements and actual scan diameter was expressed by the formula $t = p \times q \times s$, where t represents the actual scan length,

p represents the magnification factor determined by the OCT imaging system camera, q represents the magnification factor in relation to the eye, and s represents the original measurement value obtained from the OCT images. The correction factor q is expressed by the equation $q = 0.01306 \times (\text{axial length} - 1.82)$.

A single experienced operator masked to all the clinical data acquired all OCT scans. Spectral-domain OCT imaging and angiography imaging were acquired on the same day. All images were reviewed to ensure proper segmentation of the OCT scans. Scans with signal strength indices less than 70, segmentation errors, or significant motion artifacts were excluded.

• **STATISTICAL ANALYSIS:** SPSS version 19.0 (SPSS, Chicago, Illinois, USA) and R version 3.3.1 were used for all statistical analyses. Agreement on the ovality index, horizontal tilt angle, areas of the optic disc and β-zone PPA, cup-to-disc area ratio, and subfoveal choroidal thickness between 2 observers (M.S.S. and H.H.) were assessed using the Bland-Altman method, which plots their means against their differences.[31] The limits of agreement were defined as the mean differences of 2 measurements ± 1.96 standard deviations (SDs) of the difference. The normality of distribution was verified using the Shapiro-Wilk normality test, and parametric or nonparametric tests were subsequently used. Comparisons between the high myopia and control groups were performed using χ^2, independent t, or Mann-Whitney U tests, as appropriate. Paired t tests were used to compare paired data. Pearson correlation coefficients and multivariable linear regression analyses were used to investigate the association between the ocular variables and the average peripapillary vessel density and areas of surperficial and deep FAZs. All variables with a significance level of less than 0.10 in univariable analyses were included in the multivariable models. Both standardized regression coefficients and adjusted coefficients of determination (R^2) were calculated from the multivariable linear regression models after excluding variables that showed multicollinearity. Reported P values were adjusted to control the false discovery rate using the Benjamini-Hochberg procedure.[32] Further analyses involving the subgrouping of highly myopic eyes, by quartiles of horizontal tilt angle, were performed. Comparisons between the lower- and upper-quartile groups and the control group were performed using Kruskal-Wallis tests with Bonferroni-Dunn multiple comparisons for post hoc analyses. Statistical significance was considered as $P < .05$.

RESULTS

AMONG 105 SUBJECTS WHO MET THE INCLUSION CRITERIA, 8 were excluded because of unacceptable OCT image quality. As a result, 71 eyes of 71 subjects with high myopia and 26 eyes of 26 subjects with emmetropia (controls) were included. The inter-observer agreement determined using Bland-Altman plots, in the measurements of ovality index, horizontal tilt angle, areas of the optic disc and β-zone PPA, cup-to-disc area ratio, and subfoveal choroidal thickness for all subjects showed no systematic differences in measurements (data not shown). The demographic and clinical characteristics of study subjects are summarized in Table 1. The mean SE refractive error and axial length were −7.44 ± 1.70 D (range, −12.13 to −4.00 D) and 26.73 ± 0.63 mm (range, 26.01-27.98 mm) in the high myopia group and −0.08 ± 0.38 D (range, −0.50 to 0.50 D) and 23.46 ± 0.55 mm (range, 22.00-23.98 mm) in the control group, respectively. There were no significant differences in age, sex, IOP, central corneal thickness, cup-to-disc area ratio, or average pRNFL thickness between the highly myopic and control groups. However, highly myopic eyes had significantly smaller disc ($P = .007$), larger horizontal tilt angle ($P < .001$) and β-zone PPA ($P < .001$), thicker foveal thickness ($P = .019$), and thinner subfoveal choroidal thickness ($P < .001$) than eyes with emmetropia.

As shown in Table 2, vascular parameters using OCTA were significantly different between the 2 groups. The average peripapillary vessel density at the superficial retina was significantly lower in highly myopic than emmetropic eyes ($P = .010$). Areas of superficial and deep FAZ were larger in highly myopic eyes ($P = .001$ and $P < .001$, respectively). Superficial FAZ areas were significantly smaller than deep FAZ areas in both control and high myopia groups ($P < .001$ in both groups).

Next, Pearson correlation analyses were conducted to investigate the associations between vascular parameters and ocular variables in all study eyes. Additionally, we examined the effects of ONH deformation, such as horizontal disc tilt and β-zone PPA, on vascular parameters. The average peripapillary vessel density at the superficial retina was significantly negatively correlated with axial length ($P = .022$), ovality index ($P < .001$), horizontal tilt angle ($P = .003$), and area of β-zone PPA ($P < .001$). It was also correlated with average pRNFL ($P = .049$) thicknesses. In terms of macular vascular parameters, superficial FAZ area was negatively correlated with ovality index ($P = .036$), horizontal tilt angle ($P = .004$), average pRNFL thickness ($P < .001$), and foveal thickness ($P < .001$) (Table 3).

The results of multivariable regression analyses adjusted for age and sex are shown in Table 4. Ovality index was excluded from the analysis, as it is a surrogate measure of optic disc tilt and showed a significant multicollinearity with horizontal tilt angle. A significant multicollinearity was also found between the area of β-zone PPA and horizontal tilt angle. Therefore, these 2 parameters were entered into separate multivariable models. Multivariable analysis revealed that large horizontal tilt angle

TABLE 1. Demographic and Clinical Characteristics of Study Subjects

Variables	Control (N = 26)	High Myopia (N = 71)	*P* Value
Age (y)	23.11 ± 4.31 (20-30)	23.63 ± 4.01 (20-30)	.582[c]
Sex (male/female)	13/13	47/24	.163[b]
SE refractive error (D)	−0.08 ± 0.38 (−0.50 to 0.50)	−7.44 ± 1.70 (−12.13 to −4.00)	<.001[c]
IOP (mm Hg)	14.46 ± 2.40 (10-21)	14.48 ± 2.64 (10-21)	.977[a]
Axial length (mm)	23.46 ± 0.55 (22.00-23.98)	26.73 ± 0.63 (26.01-27.98)	<.001[c]
Central corneal thickness (μm)	557.92 ± 39.45 (500-632)	561.18 ± 38.40 (503-621)	.714[a]
Disc area (mm^2)	2.17 ± 0.36 (1.39-2.82)	1.90 ± 0.44 (1.17-3.01)	.007[a]
Cup-to-disc area ratio	0.33 ± 0.13 (0.06-0.53)	0.34 ± 0.16 (0.04-0.65)	.800[c]
Ovality index	1.21 ± 0.11 (1.03-1.40)	1.27 ± 0.14 (1.01-1.60)	.031[a]
Horizontal tilt angle (degrees)	5.95 ± 3.48 (0.52-10.45)	9.77 ± 3.00 (1.98-15.89)	<.001[a]
β-zone PPA (presence/absence)	14/12	65/6	<.001[b]
Area of β-zone PPA (mm^2)	0.36 ± 0.40 (0-1.25)	0.97 ± 0.53 (0-2.82)	<.001[c]
Average pRNFL thickness (μm)	106.38 ± 8.33 (89-123)	105.74 ± 9.12 (79-119)	.755[a]
Foveal thickness (μm)	245.73 ± 12.58 (217-267)	254.00 ± 20.23 (200-297)	.019[a]
Subfoveal choroidal thickness (μm)	304.27 ± 36.34 (246-365)	227.88 ± 53.16 (119-371)	<.001[a]

D = diopters; IOP = intraocular pressure; PPA = peripapillary atrophy; pRNFL = peripapillary retinal nerve fiber layer; SE = spherical equivalent.

Data are presented as mean ± standard deviation (range) unless otherwise indicated.

[a]Independent *t* test.

[b]χ^2 test.

[c]Mann-Whitney *U* test.

TABLE 2. Summary of Vascular Parameters Using Optical Coherence Tomography Angiography in the Study Subjects

Variables	Control (N = 26)	High Myopia (N = 71)	*P* Value[a]
Average peripapillary vessel density (%)	63.96 ± 2.67	62.13 ± 3.16	.010
Area of superficial FAZ (mm^2)	0.26 ± 0.05	0.31 ± 0.09	.001
Area of deep FAZ (mm^2)	0.34 ± 0.07	0.43 ± 0.12	<.001

FAZ = foveal avascular zone.

[a]Independent *t* test.

(P = .037) and β-zone PPA (P < .001) were associated with a lower peripapillary vessel density. Average pRNFL thickness also showed a significant positive correlation with average peripapillary vessel density (P = .037 in model 1 and P = .047 in model 2). Meanwhile, long axial length (P < .001), small horizontal tilt angle (P < .001), and thin foveal thickness (P < .001) were independently associated with a larger superficial FAZ area. A similar independent association was also found between the area of deep FAZ and ocular variables.

We further investigated the associations between axial length, horizontal tilt angle, and vascular parameters by subgrouping highly myopic eyes by quartiles of horizontal tilt angle. The quartiles were defined based on the method recommended by Joarder and Firozzaman.[33] Given the sample size in this study (n = 97), the upper and lower quartiles were defined first (upper quartile: n = 24, cut-off value = 11.39 degrees; lower quartile: n = 24, cut-off value = 6.87 degrees), and the remaining 49 individuals were evenly distributed into the second and third quartiles. All eyes included in the upper quartile group were highly myopic. Conversely, among the 24 eyes in the lower quartile group, only 12 eyes had high myopia. Finally, differences in vascular parameters among the 24 highly myopic eyes in the upper quartile group, 12 highly myopic eyes in the lower quartile group, and 26 emmetropic eyes in the control group were assessed. As shown in Figure 2, those in the upper quartile for horizontal tilt angle in the highly myopic group had significantly lower average peripapillary vessel density compared with those in the lower quartile (P = .025) and control groups (P = .019), while there was no significant difference in the average peripapillary vessel density between the lower quartile and control groups (P = .431; Figure 2, Left). Regarding the FAZ, those in the lower quartile for horizontal tilt angle in the high myopia group had significantly larger superficial and deep FAZ areas compared with those in the upper quartile (both P < .001) and control groups (both P < .001), while there were no differences in the areas of superficial and deep FAZs between the upper quartile and control groups (P = .835 and P = .492, respectively; Figure 2, Center and Right).

TABLE 3. Pearson Correlation Analysis Between Vascular Parameters Using Optical Coherence Tomography Angiography and Ocular Variables

	Average Peripapillary Vessel Density			Area of Superficial FAZ			Area of Deep FAZ		
	r	*P*	Adjusted *P*[a]	r	*P*	Adjusted *P*[a]	r	*P*	Adjusted *P*[a]
IOP	−0.102	.322	.375	−0.084	.415	.652	−0.050	.625	.764
Axial length	−0.262	.010	.022*	0.201	.049	.090	0.327	.001	.006*
Central corneal thickness	0.018	.861	.861	−0.033	.745	.770	−0.095	.353	.485
Disc area	0.190	.064	.104	0.072	.486	.668	−0.001	.994	.994
Cup-to-disc area ratio	0.159	.115	.150	0.210	.040	.088	0.237	.020	.044*
Ovality index	−0.350	<.001	<.001*	−0.252	.013	.036*	−0.168	.100	.183
Horizontal tilt angle	−0.314	.002	.003*	−0.330	.001	.004*	−0.280	.006	.022*
Area of β-zone PPA	−0.485	<.001	<.001*	0.030	.770	.770	0.105	.306	.481
Average pRNFL thickness	0.203	.047	.049*	−0.347	<.001	<.001*	−0.267	.008	.022*
Foveal thickness	−0.170	.097	.140	−0.589	<.001	<.001*	−0.341	.001	.006*
Subfoveal choroidal thickness	0.180	.164	.195	−0.202	.115	.124	−0.206	.108	.121

FAZ = foveal avascular zone; IOP = intraocular pressure; PPA = peripapillary atrophy; pRNFL = peripapillary retinal nerve fiber layer.
Factors with statistical significance are indicated by asterisk (*).
[a]*P* values adjusted with Benjamini-Hochberg procedure.

DISCUSSION

IN THE PRESENT STUDY, OCTA IMAGES OF THE PERIPAPILLARY and macular regions in eyes with high myopia were analyzed. We found a decrease in peripapillary vessel density and enlargement of the superficial and deep FAZs in highly myopic eyes. We also demonstrated strong correlations between horizontal disc tilt and vascular parameters, such as peripapillary vessel density and area of the FAZ. To our knowledge, this is the first investigation of the association between ONH deformation and retinal microvasculature in myopia.

Demographic characteristics of highly myopic eyes revealed in the current study are in accordance with the previous reports.[34–37] Highly myopic eyes had smaller optic disc and larger disc tilt and β-zone PPA. In addition, they had thicker fovea compared with emmetropic eyes. Lim and associates[36] proposed that this association is a result of overestimations of foveal thickness owing to poorer and off-fovea fixation in highly myopic eyes. However, for all subjects in the present study, we have checked the central alignment during macular OCT imaging; therefore the effects of off-fovea fixation might be negligible. Alternatively, we agree with the suggestion of Wu and associates[37] that the flattening tendency of the ILM and centripetal force of the posterior vitreous induced by stretching of sclera result in elevation of fovea.

Several studies have reported the conflicting findings regarding the microcirculatory states in healthy myopia. Li and associates[9] and Yang and associates[10] described the decrease of superficial and deep macular microvascular density in high myopia without noticeable degenerative retinopathy. Fan and associates[11] also showed that, with increases in axial length, macular region vascular density decreased. On the other hand, Mo and associates[38] reported that vascular density in the macular region was not significantly different between healthy high myopia and emmetropia groups. Benavente-Pérez and associates[6] also found no significant differences in the capillary circulation of the macular region using the Heidelberg retina flowmeter. Regarding peripapillary microvasculature, Wang and associates[13] described decreased peripapillary retinal perfusion in high myopia, but they could not find a difference in parafoveal retinal perfusion between myopic and emmetropic eyes. In the current study, highly myopic eyes generally exhibited lower average peripapillary vessel density and larger FAZ compared to emmetropic eyes, suggesting decreased peripapillary and macular perfusion.

The mechanism of decreased retinal blood flow and perfusion in myopic eyes remains unclear. Presumably, with axial elongation and expansion of the eyeball in highly myopic eyes, retinal vessels may be straightened and attenuated, which results in decreased blood flow and perfusion. In addition, thinning of the RNFL may affect regional oxygen demand or the need for vascular supply, thereby triggering retinal vascular adjustment via autoregulatory mechanisms. Our findings and hypothesis are in line with the study by La Spina and associates,[39] who found that the myopic posterior pole presents a reduced diameter of vascular network, but is functionally comparable to control eyes. Their result supports the hypothesis of reduced oxygen consumption in highly myopic eyes.

An RPC comprises a distinct network of capillary beds located within the RNFL that supply the retinal ganglion cell (RGC) axons. In accordance with previous reports,[40,41]

TABLE 4. Linear Regression Analysis With Average Peripapillary Vessel Density and Area of Superficial and Deep Foveal Avascular Zone as Dependent Variables

	Univariable Analysis[a]			Multivariable Analysis[a]			
Variables	Coefficient	R^{2b}	*P* Value[c]	Coefficient	*P* Value[c]	Coefficient	*P* Value[c]
Average peripapillary vessel density				Model 1 ($R^2 = 0.134$[b])		Model 2 ($R^2 = 0.254$[b])	
Axial length	−0.236	0.061	.027	−0.101	.737	−0.008	.406
Ovality index	−0.356	0.135	<.001	-	-	-	-
Horizontal tilt angle	−0.304	0.101	.003	−0.265	.037*	-	-
Area of β-zone PPA	−0.499	0.250	<.001	-	-	−0.479	<.001*
Average pRNFL thickness	0.205	0.044	.069	0.216	.037*	0.197	.047*
Area of superficial FAZ				$R^2 = 0.533$[b]			
Axial length	0.203	0.013	.085	0.479	<.001*		
Cup-to-disc area ratio	0.207	0.013	.080	−0.026	.826		
Ovality index	−0.249	0.036	.031	-	-		
Horizontal tilt angle	−0.332	0.085	.004	−0.462	<.001*		
Average pRNFL thickness	−0.365	0.095	.004	−0.144	.096		
Foveal thickness	−0.617	0.353	<.001	−0.530	<.001*		
Area of deep FAZ				$R^2 = 0.414$[b]			
Axial length	0.328	0.099	.003	0.588	<.001*		
Cup-to-disc area ratio	0.217	0.034	.061	0.009	.931		
Horizontal tilt angle	−0.281	0.072	.011	−0.462	<.001*		
Average pRNFL thickness	−0.244	0.046	.042	−0.100	.336		
Foveal thickness	−0.377	0.134	<.001	−0.268	.010*		

FAZ = foveal avascular zone; PPA = peripapillary atrophy; pRNFL = peripapillary retinal nerve fiber layer.
Variables with significance of $P > .1$ in the univariable analysis were not shown in this table.
Factors with statistical significance are indicated by asterisk (*).
[a]Adjusted for age and sex.
[b]Adjusted R^2 from the fitted model.
[c]*P* values adjusted with Benjamini-Hochberg procedure.

we found positive correlations between average peripapillary vessel density and average pRNFL thicknesses in univariable analysis. We also observed negative correlations between average peripapillary vessel density and axial length and parameters of ONH deformation, such as ovality index, horizontal tilt angle, and area of β-zone PPA. However, multivariable analyses revealed that average peripapillary vessel density significantly associated only with average pRNFL thickness and parameters of ONH deformation. Since the metabolic demands of RGC axons are met by the RPCs, the decrease in peripapillary vessel density in eyes with large horizontal disc tilt or β-zone PPA may be caused by a reduced blood supply demand owing to peripapillary retinal changes. In addition, it is also possible that the direct mechanical damage to the peripapillary microvasculature during the development of ONH deformation might contribute to a decrease in peripapillary vessel density.

Various demographic and ocular factors are known to influence the FAZ area. Among several potential factors, the influence of foveal thickness on FAZ area has been well described by previous studies.[15,42] In the current study, we found increases in foveal thickness with axial elongation, and a strong negative correlation between foveal thickness and the areas of superficial and deep FAZs. Samara and associates[42] suggest that the variability in the FAZ area with changing foveal thickness may be explained by foveal development. Deeper foveal pits result in a wider separation of the superficial retinal layers and, hence, larger FAZs.

Only a few studies have reported a change in the FAZs of myopic eyes. Recently, Tan and associates[15] demonstrated that axial length did not significantly affect FAZ area after adjusting for central retinal thickness and sex. Chui and associates[43] also reported no relationship between the FAZ areas and axial length. However, these studies did not consider the ocular magnification effect in measuring the FAZ. In the current study, the FAZ areas of myopic eyes were adjusted by the scaling factor from Bennett's formula; we found that superficial and deep FAZ areas were larger in eyes with greater myopia. One explanation, as mentioned earlier, may be that decreased regional oxygen demand in myopic eyes results in enlargement of FAZs. Alternatively, mechanical stretching of the FAZ by axial elongation may partly account for the FAZ enlargement.

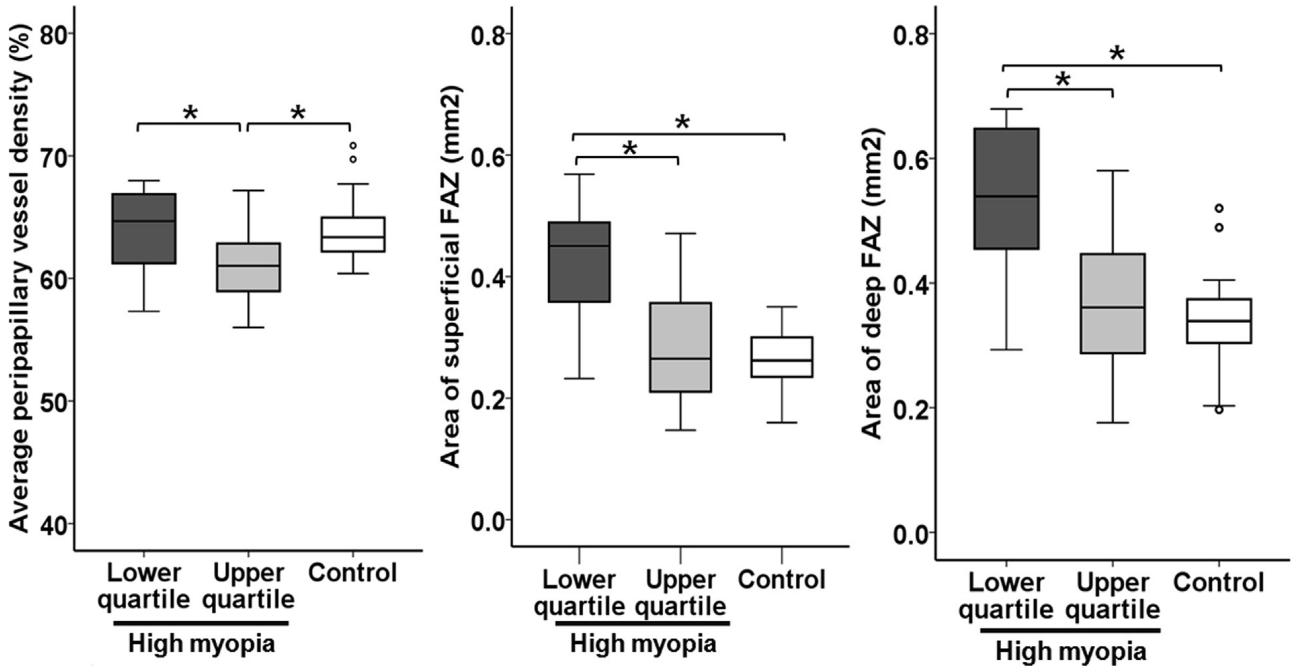

FIGURE 2. Box-whisker plots demonstrating average peripapillary vessel density (Left) and the areas of superficial (Center) and deep (Right) foveal avascular zone in normal controls and lower and upper quartile highly myopic groups based on horizontal tilt angle. *Statistically significant difference ($P < .05$)

Interestingly, we found significant differences in the vascular parameters of highly myopic eyes according to the degree of horizontal disc tilt. The FAZ areas decreased with increases in horizontal tilt angle. Highly myopic eyes with large disc tilt showed decreased peripapillary microvasculature compared to emmetropic eyes, whereas the FAZ was preserved. Conversely, highly myopic eyes without definitive disc tilt showed enlargement of the FAZ, which means decreased foveal microvasculature, whereas peripapillary vessel densities were comparable to those of emmetropic eyes.

Recently, Sawada and associates[44,45] reported that ONH deformation such as optic disc tilt, but not refractive error itself, is related to the degree of VF defects and rate of VF progression in myopic glaucoma. These studies suggest that the potential effect of ONH deformation should be considered when evaluating retinal structural alterations in myopic eyes. Similarly, the current result, that eyes with larger myopic optic disc tilt are associated with the preservation of the FAZ, led us to hypothesize that the configuration of ONH may influence microvasculature not only in the peripapillary regions but also macular regions in highly myopic eyes. In addition, our findings suggest that the inconsistent results, in terms of the microvasculature of myopic eyes shown by previous studies, may be attributable to differences in the degree of ONH deformation of included myopic subjects. Most previous studies did not consider the ONH characteristics when interpreting the microvasculature changes in myopic eyes.

The mechanism behind the association between optic disc tilt and FAZ is unclear. We suggest that our findings could be explained in part by regional differences in scleral stress. A previous histomorphometric study revealed that scleral thinning occurred posterior to the equator, markedly closer to the posterior pole, in eyes with axial elongation.[46] This finding suggests that mechanical stress by scleral stretching is predominantly loaded on the posterior pole region. In highly myopic eyes with large disc tilt, this mechanical stress might be relieved, to some degree, by ONH deformation, and therefore, local strain of the foveal region might be relatively decreased. Conversely, in highly myopic eyes without definitive disc tilt, mechanical stress loaded on the posterior pole region cannot be relieved, and the FAZs are consequently enlarged. Although the reason why some of the highly myopic eyes present ONH deformation while others do not is still not clear, it may be related to the distributions of stress, strain, and deformation that are determined by the complex material properties and geometries of sclera and lamina cribrosa. Thus, studies regarding the biomechanical properties of sclera warrant further investigation in high myopia.

Choroidal thinning is one of the important features in high myopia. We found a significant thinning of subfoveal choroid in highly myopic eyes. Considering that a presumed mechanism for choroidal thinning in highly myopic eyes is also the mechanical stretching during axial elongation, one might expect to find some associations between subfoveal choroid and FAZ. However, there was no

significant correlation between the subfoveal choroidal thickness and FAZ area in the current study. Our finding indicates that mechanical stretching is not likely to be the sole mechanism, and other factors might be involved in the subfoveal choroidal thinning and FAZ enlargement in high myopia.

The major limitation of this study was the small number of examined eyes. We employed strict inclusion criteria to assess the exclusive influence of axial myopia. These criteria resulted in the exclusion of a certain proportion of potential subjects, thus decreasing the sample size. Therefore, our findings may not be extrapolated to extremely high myopia or pathologic myopia. A larger population study is recommended to increase the robustness of our data. In addition, we did not evaluate the sclera or lamina cribrosa. To determine the underlying mechanisms of the association between myopia and ocular blood flow, it would be useful to measure scleral thickness and the lamina cribrosa in future studies.

In conclusion, we found significant reductions in the peripapillary and macular microvasculature of highly myopic eyes. In addition, there were significant differences in the microvasculature, by degree of ONH deformation, of highly myopic eyes. We believe that our findings may provide new insights into the pathomechanisms of various ophthalmic diseases in myopia.

FUNDING/SUPPORT: THIS RESEARCH WAS SUPPORTED BY THE BASIC SCIENCE RESEARCH PROGRAM THROUGH THE NATIONAL Research Foundation (NRF) of Korea, funded by the Ministry of Education (NRF-2015R1D1A1A01059630), and the Bio & Medical Technology Development Program of the NRF, funded by the Ministry of Science and ICT (MSIT) (NRF-2017M3A9E8023019). The funding organizations had no role in the design or conduct of this research. Financial Disclosures: The following authors have no financial disclosures: Mi Sun Sung, Tae Hee Lee, Hwan Heo, and Sang Woo Park. The authors attest that they meet the current ICMJE criteria for authorship.

REFERENCES

1. Avetisov ES, Savitskaya NF. Some features of ocular microcirculation in myopia. *Ann Ophthalmol* 1977;9(10):1261–1264.
2. Shimada N, Ohno-Matsui K, Harino S, et al. Reduction of retinal blood flow in high myopia. *Graefes Arch Clin Exp Ophthalmol* 2004;242(4):284–288.
3. Gopinath B, Wang JJ, Kifley A, Tan AG, Wong TY, Mitchell P. The association between ocular biometry and retinal vascular caliber is comparable from early childhood to adolescence. *Invest Ophthalmol Vis Sci* 2013;54(2):1501–1508.
4. Tai EL, Li LJ, Wan-Hazabbah WH, Wong TY, Shatriah I. Effect of axial eye length on retinal vessel parameters in 6 to 12-year-old Malay girls. *PLoS One* 2017;12(1):e0170014.
5. Wong TY, Knudtson MD, Klein R, Klein BE, Meuer SM, Hubbard LD. Computer-assisted measurement of retinal vessel diameters in the Beaver Dam Eye Study: methodology, correlation between eyes, and effect of refractive errors. *Ophthalmology* 2004;111(6):1183–1190.
6. Benavente-Pérez A, Hosking SL, Logan NS, Broadway DC. Ocular blood flow measurements in healthy human myopic eyes. *Graefes Arch Clin Exp Ophthalmol* 2010;248(11):1587–1594.
7. Lee TH, Heo H, Park SW. Clinical usefulness of spectral-domain optical coherence tomography in glaucoma and NAION. *Chonnam Med J* 2016;52(3):194–200.
8. Al-Sheikh M, Phasukkijwatana N, Dolz-Marco R, et al. Quantitative OCT angiography of the retinal microvasculature and the choriocapillaris in myopic eyes. *Invest Ophthalmol Vis Sci* 2017;58(4):2063–2069.
9. Li M, Yang Y, Jiang H, et al. Retinal microvascular network and microcirculation assessments in high myopia. *Am J Ophthalmol* 2017;174:56–67.
10. Yang Y, Wang J, Jiang H, et al. Retinal microvasculature alteration in high myopia. *Invest Ophthalmol Vis Sci* 2016;57(14):6020–6030.
11. Fan H, Chen HY, Ma HJ, et al. Reduced macular vascular density in myopic eyes. *Chin Med J (Engl)* 2017;130(4):445–451.
12. Wang X, Zheng Y, Kong X, Zhu L, Sun X. The characteristics of peripapillary retinal perfusion by optical coherence tomography angiography in tessellated fundus eyes. *PLoS One* 2016;11(7):e0159911.
13. Wang X, Kong X, Jiang C, Li M, Yu J, Sun X. Is the peripapillary retinal perfusion related to myopia in healthy eyes? A prospective comparative study. *BMJ Open* 2016;6(3):e010791.
14. Iafe NA, Phasukkijwatana N, Chen X, Sarraf D. Retinal capillary density and foveal avascular zone area are age-dependent: Quantitative analysis using optical coherence tomography angiography. *Invest Ophthalmol Vis Sci* 2016;57(13):5780–5787.
15. Tan CS, Lim LW, Chow VS, et al. Optical coherence tomography angiography evaluation of the parafoveal vasculature and its relationship with ocular factors. *Invest Ophthalmol Vis Sci* 2016;57(9):224–234.
16. Balaratnasingam C, Inoue M, Ahn S, et al. Visual acuity is correlated with the area of the foveal avascular zone in diabetic retinopathy and retinal vein occlusion. *Ophthalmology* 2016;123(11):2352–2367.
17. Kwon J, Choi J, Shin JW, Lee J, Kook MS. Alterations of the foveal avascular zone measured by optical coherence tomography angiography in glaucoma patients with central visual field defects. *Invest Ophthalmol Vis Sci* 2017;58(3):1637–1645.
18. Ohno-Matsui K. Proposed classification of posterior staphylomas based on analyses of eye shape by three-dimensional magnetic resonance imaging. *Ophthalmology* 2014;121(9):1798–1809.

19. Ohno-Matsui K, Akiba M, Moriyama M, et al. Acquired optic nerve and peripapillary pits in pathologic myopia. *Ophthalmology* 2012;119(8):1685–1692.
20. Morgan IG, Ohno-Matsui K, Saw SM. Myopia. *Lancet* 2012; 379(9827):1739–1748.
21. Samarawickrama C, Mitchell P, Tong L, et al. Myopia-related optic disc and retinal changes in adolescent children from singapore. *Ophthalmology* 2011;118(10):2050–2057.
22. Sung MS, Kang YS, Heo H, Park SW. Characteristics of optic disc rotation in myopic eyes. *Ophthalmology* 2016;123(2): 400–407.
23. Sung MS, Kang YS, Heo H, Park SW. Optic disc rotation as a clue for predicting visual field progression in myopic normal-tension glaucoma. *Ophthalmology* 2016;123(7):1484–1493.
24. Bennett AG, Rudnicka AR, Edgar DF. Improvements on Littmann's method of determining the size of retinal features by fundus photography. *Graefes Arch Clin Exp Ophthalmol* 1994;232(6):361–367.
25. Cheung SW, Cho P, Douthwaite W. Corneal shape of Hong Kong-Chinese. *Ophthalmic Physiol Opt* 2000;20(2):119–125.
26. Kang SH, Hong SW, Im SK, Lee SH, Ahn MD. Effect of myopia on the thickness of the retinal nerve fiber layer measured by Cirrus HD optical coherence tomography. *Invest Ophthalmol Vis Sci* 2010;51(8):4075–4083.
27. Hosseini H, Nassiri N, Azarbod P, et al. Measurement of the optic disc vertical tilt angle with spectral-domain optical coherence tomography and influencing factors. *Am J Ophthalmol* 2013;156(4):737–744.
28. Park HY, Choi SI, Choi JA, Park CK. Disc torsion and vertical disc tilt are related to subfoveal scleral thickness in open-angle glaucoma patients with myopia. *Invest Ophthalmol Vis Sci* 2015;56(8):4927–4935.
29. Jia Y, Tan O, Tokayer J, et al. Split-spectrum amplitude-decorrelation angiography with optical coherence tomography. *Opt Express* 2012;20(4):4710–4725.
30. Linderman R, Salmon AE, Strampe M, Russillo M, Khan J, Carroll J. Assessing the accuracy of foveal avascular zone measurements using optical coherence tomography angiography: segmentation and scaling. *Transl Vis Sci Technol* 2017;6(3):16.
31. Bland JM, Altman DG. Statistical methods for assessing agreement between two methods of clinical measurement. *Lancet* 1986;1(8476):307–310.
32. Benjamini Y, Hochberg Y. Controlling the false discovery rate: a practical and powerful approach to multiple testing. *J R Stat Soc B* 1995;57(1):289–300.
33. Joarder AH, Firozzaman M. Quartiles for discrete data. *Teaching Statistics* 2001;23(3):86–89.
34. Koh V, Tan C, Tan PT, et al. Myopic maculopathy and optic disc changes in highly myopic young Asian eyes and impact on visual acuity. *Am J Ophthlamol* 2016;164:69–79.
35. Gupta P, Sidhartha E, Tham YC, et al. Determinants of macular thickness using spectral domain optical coherence tomography in healthy eyes: the Singapore Chinese Eye study. *Invest Ophthalmol Vis Sci* 2013;54(13): 7968–7976.
36. Lim MC, Hoh ST, Foster PJ, et al. Use of optical coherence tomography to assess variations in macular retinal thickness in myopia. *Invest Ophthalmol Vis Sci* 2005; 46(3):974–978.
37. Wu PC, Chen YJ, Chen CH, et al. Assessment of macular retinal thickness and volume in normal eyes and highly myopic eyes with third-generation optical coherence tomography. *Eye (Lond)* 2008;22(4):551–555.
38. Mo J, Duan A, Chan S, Wang X, Wei W. Vascular flow density in pathological myopia: an optical coherence tomography angiography study. *BMJ Open* 2017;7(2):e013571.
39. La Spina C, Corvi F, Bandello F, Querques G. Static characteristics and dynamic functionality of retinal vessels in longer eyes with or without pathologic myopia. *Graefes Arch Clin Exp Ophthalmol* 2016;254(5):827–834.
40. Mammo Z, Heisler M, Balaratnasingam C, et al. Quantitative optical coherence tomography angiography of radial peripapillary capillaries in glaucoma, glaucoma suspect, and normal eyes. *Am J Ophthalmol* 2016;170:41–49.
41. Yarmohammadi A, Zangwill LM, Diniz-Filho A, et al. Optical coherence tomography angiography vessel density in healthy, glaucoma suspect, and glaucoma eyes. *Invest Ophthalmol Vis Sci* 2016;57(9):451–459.
42. Samara WA, Say EA, Khoo CT, et al. Correlation of foveal avascular zone size with foveal morphology in normal eyes using optical coherence tomography angiography. *Retina* 2015; 35(11):2188–2195.
43. Chui TY, VanNasdale DA, Elsner AE, Burns SA. The association between the foveal avascular zone and retinal thickness. *Invest Ophthalmol Vis Sci* 2014;55(10):6870–6877.
44. Sawada Y, Hangai M, Ishikawa M, Yoshitomi T. Association of myopic optic disc deformation with visual field defects in paired eyes with open-angle glaucoma: a cross-sectional study. *PLoS One* 2016;11(8):e0161961.
45. Sawada Y, Hangai M, Ishikawa M, Yoshitomi T. Association of myopic deformation of optic disc with visual field progression in paired eyes with open-angle glaucoma. *PLoS One* 2017;12(1):e0170733.
46. Vurgese S, Panda-Jonas S, Jonas JB. Scleral thickness in human eyes. *PLoS One* 2012;7(1):e29692.